On-line Continuous Measurement of the Operating Deflection Shape of Power Transmission Belts through Electrostatic Sensing

Yonghui Hu[a], Lu Yang[a], Lijuan Wang[a,b], Xiangchen Qian[a], Yong Yan[b]
[a] School of Control and Computer Engineering
North China Electric Power University, Beijing 102206, P. R. China
[b] School of Engineering and Digital Arts
University of Kent, Canterbury, Kent CT2 7NT, U. K.

***Abstract*—The measurement of the operating deflection shape (ODS) of power transmission belts is of great importance for the fault diagnosis and prognosis of industrial belt drive systems. This paper presents a novel method based on an electrostatic sensor array to measure the ODS of a belt moving both axially and transversely. Finite element simulations are performed to study the sensing characteristics of a strip-shaped electrode and the results reveal that the transverse velocity determines the sensor signal. Construction of the ODS is achieved in the frequency domain using the ODS frequency response function. Experiments conducted on a purpose-built test rig show that the belt vibrates at resonant frequencies that are well separated and identifiable using a peak picking method. The ODSs for different vibration modes exhibit similar deformation patterns and the axial motion of the belt determines that the ODSs propagate along the belt length, rather than stay fixed in space.**

Keywords— Belt drive; vibration measurement; electrostatic sensor; sensor array; operating deflection shape; frequency response function.

I. INTRODUCTION

Belt drives are extensively used to transmit power between shafts in a variety of industrial, automotive, agricultural and home appliance applications. They are frequently preferred to chains and gears because of simple installation, low maintenance, misalignment tolerance and shock absorption. However, the axially moving belt is prone to vibrations due to the compliance of the material. In addition, a variety of mechanical defects, such as shaft misalignment, pulley eccentricity, belt wear and improper belt tensioning, may give rise to excessive belt vibrations that cause noise radiation, belt fatigue, speed loss and possibly a catastrophic machine failure [1, 2]. In order to monitor the dynamic behaviors of the belt and diagnose machinery problems, it is desirable to measure and characterize the belt vibration on an on-line continuous basis.

A powerful technique for vibration characterization is operating deflection shape (ODS) analysis. ODS can be defined as the deflection of a structure at a particular frequency, or more generally as any forced motion of two or more degrees of freedom on a structure [3, 4]. In contrast with mode shape that characterizes only the resonant vibration of a structure, ODS contains both forced and resonant vibration components. Therefore, ODS analysis enables visualization of the deformation pattern of a structure or machine functioning under normal operating conditions. To construct an ODS, the vibrations at multiple locations of the structure are measured simultaneously. The vibration magnitude and phase of all points define an ODS vector, which can be used for shape animation of the structure. ODS analysis of a power transmission belt is particularly useful in the study of its complex vibration behaviors. The knowledge about the deflection along the length of the belt facilitates the determination of vibration spatial distribution and the troubleshooting of abnormal vibrations without any machine downtime.

In the last few decades, there has been considerable research on the vibration of power transmission belts. However, the majority of studies have focused on dynamic modelling and theoretical analysis [5, 6], and little research has been undertaken on vibration measurement and ODS analysis, which has been regarded as a challenging task, especially for long-term industrial applications. The axial motion of the belt precludes the employment of conventional contact type sensors such as accelerometers and strain gages. It is also difficult to adapt the various proximity probes developed for the deviation detection of a rotating shaft to the measurement of belt vibration. Catalano *et al.* [7] carried out vibration analysis of a belt system using a high-speed camera, which recorded the positions of marked points on the belt. However, on-line continuous measurement cannot be realized using this technique due to the high computational overhead required. Xia *et al.* [8] employed two laser displacement sensors to monitor the vertical and horizontal vibrations of an axially moving string. Agnani *et al.* [9] experimentally investigated the belt vibration behaviors using single-point laser Doppler vibrometers (LDV). Sante and Rossi [10] measured the ODS of a synchronous belt using a scanning LDV for the development of a vibro-acoustic model. The laser-based technique can perform non-contact vibration measurement with high sensitivity and high spatial resolution; however, such instruments are prohibitively expensive to implement in routine industrial applications and the use of delicate optical components limits their applicability in dusty, harsh and extreme environments.

In our previous studies [11, 12], it was found that a dielectric belt running on earthed metal rollers carries electrostatic charge due to contact and frictional electrification. Information about the motion of the belt can be derived using electrostatic sensors placed adjacent to the belt. Specifically, the transverse vibration of the belt can be measured by analyzing the spectrum of the electrostatic signal. The electrostatic sensor is simple, non-contact, inexpensive and

suitable for hostile environments, thus representing an appealing solution to the belt vibration measurement problem in industry. This paper establishes the relationship between the sensor signal and the transverse velocity of the belt through finite element modelling and extends the single-point measurement to ODS measurement using a sensor array. The fundamental principle, finite element modelling, practical design, implementation and experimental assessment of the measurement system are presented.

II. Measurement Principle

A. Sensing Arrangement

The amount of electrostatic charge generated on the belt surface depends on a variety of factors including roller speed, belt tension, ambient temperature and humidity. For fixed operating and environment conditions, the distribution of charge on the belt surface is mainly affected by the surface roughness. Since the non-uniformity of surface charge distribution is very small, the fluctuation of the electric field around the belt is dominated by the transverse vibration of the belt. Therefore, the amount of induced charge on a metal electrode located in the proximity of the belt varies along with its distance to the belt. Due to the localized sensing zone, the electrostatic sensor measures belt vibration at only a single point. In order to obtain an ODS measurement, multiple sensors arranged in a linear array along the belt length are employed. Fig. 1 illustrates the sensing arrangement and principle of the measurement system.

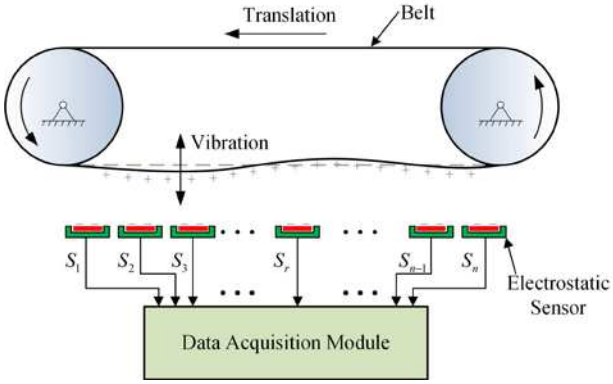

Fig. 1. Sensing arrangement and principle of the measurement system.

B. Vibration Measurement

In order to interpret how the electrostatic sensor responds to the belt vibration, finite element simulations are performed using the commercial software package COMSOL Multiphysics. In comparison with the theoretical modelling approach [13], finite element simulations provide efficient numerical solutions to the electrostatic boundary-value problem without solving any equations. In view of the superposition principle of electric field, a point charge that vibrates harmonically in the normal direction of the electrode surface is configured in the modelling. Fig. 2 shows the finite element model finely meshed with tetrahedral elements. The electrode is modelled as a thin copper strip with dimensions of 20 mm in length and 3 mm in width. The point charge is assumed to carry net electrostatic charge of -1 μC. The total induced charge on the electrode is obtained through integration of the surface charge density.

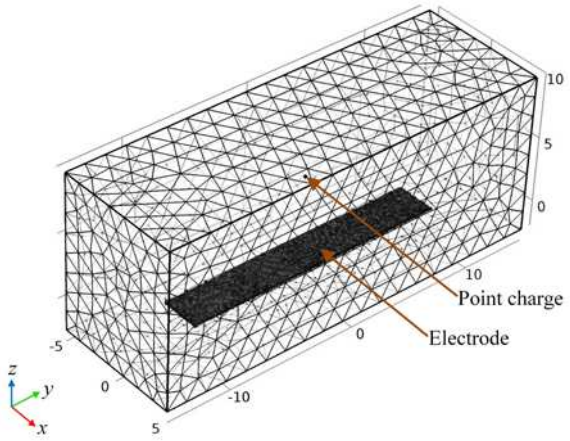

Fig. 2. Finite element model of the electrostatic sensor.

The center of the electrode is located at the origin of the coordinate system, as shown in Fig. 2. The harmonic motion of the point charge is described by

$$z = 6 + A\sin(2\pi ft) \tag{1}$$

where A denotes the vibration amplitude and f the vibration frequency. In this study the distance from the electrode to the equilibrium position of the point charge is set as 6 mm, which is not too far in order to obtain enough induced charge and not too near in order to avoid a sharp increase of induced charge when the point charge approaches the electrode. The output of the electrode is a current signal that is the time derivative of the induced charge, i.e.

$$I = \frac{dq}{dt} \tag{2}$$

where I is the current output and q the induced charge.

Fig. 3 depicts the induced charge and corresponding current output for different vibration amplitudes and frequencies. As can be seen, the electrode generates more current for a larger vibration amplitude, under which a longer excursion distance is covered and the variation of the induced charge is stronger. It is also observed that the amplitude of the alternating current output increases with the vibration frequency. If the variation of the induced charge can be approximated using a sinusoidal function, it is easy to understand, from a mathematical point of view, that the amplitude of its time derivative (the current) is proportional to the frequency (eq. (1) and (eq.(2)).

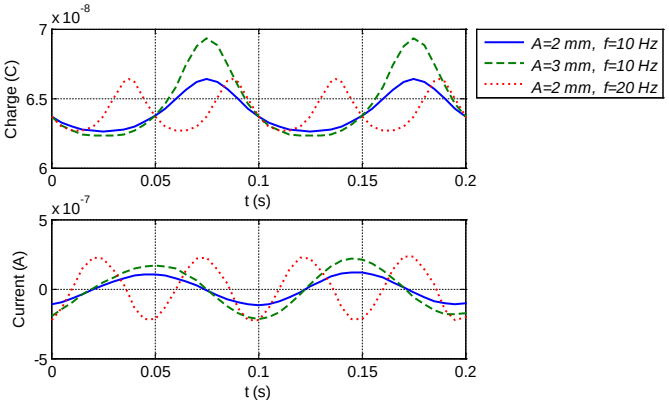

Fig. 3. Induced charge and corresponding current output for different vibration amplitudes and frequencies.

The simulation results shown in Fig. 3 reveal that the transverse velocity of the belt determines the sensor signal. However, the absolute value of the transverse velocity cannot be measured using the electrostatic sensor output due to the vulnerability of the electrostatic sensing technique to environmental and operating conditions. It is also worth noting that the transverse velocity is positively, but nonlinearly related to the sensor signal amplitude due to the non-uniform spatial sensitivity of the sensor [13]. Nevertheless, quantitative characterization of the belt vibration can be achieved through spectral analysis of the sensor signal.

C. ODS Measurement

An ODS can be derived from a set of time domain signals acquired simultaneously or frequency domain measurements that are computed from the time domain signals [4, 14]. Among the various techniques available, the ODS frequency response function (FRF) is used to construct the ODS in this study. This technique requires a fixed reference sensor in order to determine the relative phase of each measurement point. To calculate an ODS FRF, the magnitude of the cross spectrum between a sensor signal and the reference sensor signal is replaced with the auto spectrum of the sensor signal. In this way, the correct magnitude of the sensor signal and the correct phase relative to the reference signal are retained. The definition of the ODS FRF is given by the following equation [15]:

$$H_i(\omega) = S_i(\omega)S_i^*(\omega)\bullet\frac{S_i(\omega)S_r^*(\omega)}{|S_i(\omega)S_r^*(\omega)|} \tag{3}$$

where $S_i(\omega)$ and $S_r(\omega)$ represent the Fourier transform of the *i*-th sensor signal $s_i(t)$ and the reference signal $s_r(t)$, respectively. The operator $*$ denotes the complex conjugate. The first term in equation (3) represents the auto spectrum of the *i*-th sensor signal and the second term the phase of the cross spectrum between the *i*-th sensor signal and the reference signal.

Under the conditions of low damping and well-separated vibration modes, the ODS FRFs reach a local maximum around the resonant frequencies, which can be identified using the so-called peak picking (PP) method [16]. Since the response of the electrostatic sensor represents the transverse velocity, the real components of the ODS FRFs at resonant frequency ω_i are assembly as follows to yield the *i*-th mode shape vector φ_i [13]:

$$\varphi_i = \begin{Bmatrix} \mathrm{Re}[H_1(\omega_i)] \\ \mathrm{Re}[H_2(\omega_i)] \\ \vdots \\ \mathrm{Re}[H_r(\omega_i)] \\ \vdots \\ \mathrm{Re}[H_n(\omega_i)] \end{Bmatrix} \tag{4}$$

where *n* is the number of sensors deployed, with one of them being the reference sensor.

III. Experiental Results and Discussion

A. Experimental Setup

The electrostatic sensor is a two-layer printed circuit board that consists of an electrode as a long surface-mount pad on the bottom layer and the signal conditioning circuit on the top layer [12]. A total of 20 electrostatic sensors with an equal spacing of 20 mm between adjacent elements form a linear array. Fig. 4 shows the electrostatic sensor array. The sensor signals were sampled simultaneously at a frequency of 50 kHz using a data acquisition (DAQ) module (National Instruments, model USB-6363) and processed on a host computer.

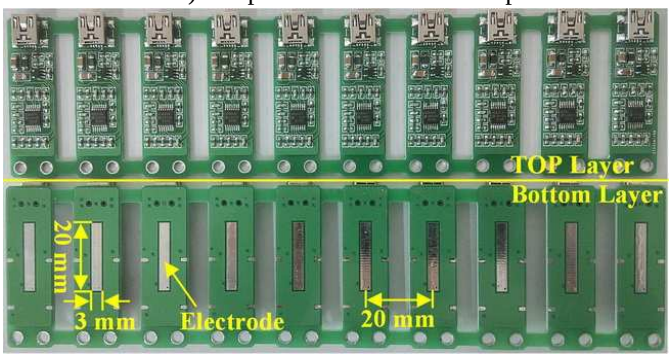

Fig. 4. Part of the electrostatic sensor array.

Experiments with the measurement system were conducted on a custom-built test rig, as shown in Fig. 5. The rig consists of a flat, nylon-type belt and two earthed metal pulleys with an equal diameter. The axial speed of the belt can be adjusted by regulating the rotational speed of a driving motor. As the center-to-center distance between the two pulleys is 390 mm, the sensor array covers almost the whole slack side of the belt span. The distance from the sensor array to the belt in stationary state is set as 15 mm.

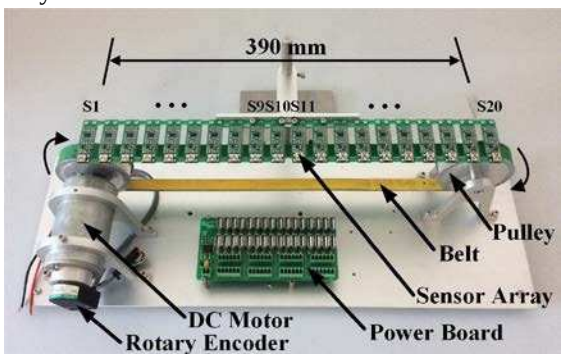

Fig. 5. Test rig.

B. Vibration Measurement Results

Fig. 6 shows five typical signal waveforms from sensors S_1, S_9, S_{10}, S_{11} and S_{20}, as labelled in Fig. 5, when the belt axial speed is 6 m/s. Signals S_9, S_{10}, and S_{11} are from sensors in the middle of the belt. It is evident that a downstream signal is a time-delayed but corrupted version of its preceding one. If the belt vibration can be regarded as a travelling wave that propagates along the belt length, the sensors in the array experience different phases of the travelling wave, leading to the phase shifts observed in the signals. The amplitudes of the signals s_1 and s_{20} at both ends are smaller than the others, because of the small vibration displacement close to the pulley.

It is also observed that there are strong spikes in s_{20}, which is believed to be due to the electrostatic discharge when the belt and pulley come into contact.

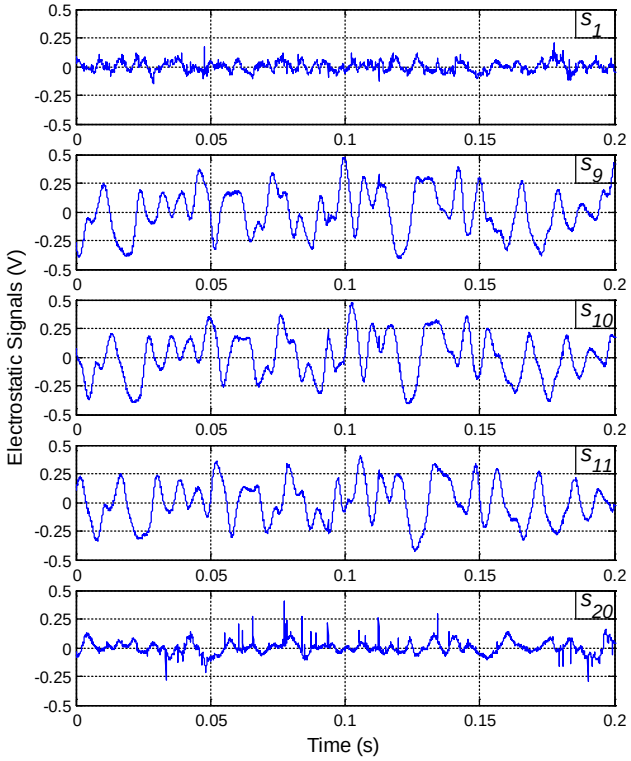

Fig. 6. Signals from sensors S_1, S_9, S_{10}, S_{11} and S_{20} at a belt axial speed of 6 m/s.

The amplitude spectra of the electrostatic signals in Fig. 6, but of a longer period of time (2s), are plotted in Fig. 7. It is illustrated that there exist strong, well-separated spectral peaks at the same frequencies in all signals. These vibration frequencies satisfy an integer multiple relationship with the fundamental frequency, and thus can be regarded as the resonant frequencies identifiable using the PP method. It is also shown that the signals share almost the same relative magnitude of the spectral peaks. Note that the spikes in s_{20} are much higher than 150 Hz and hence not visible in the spectra.

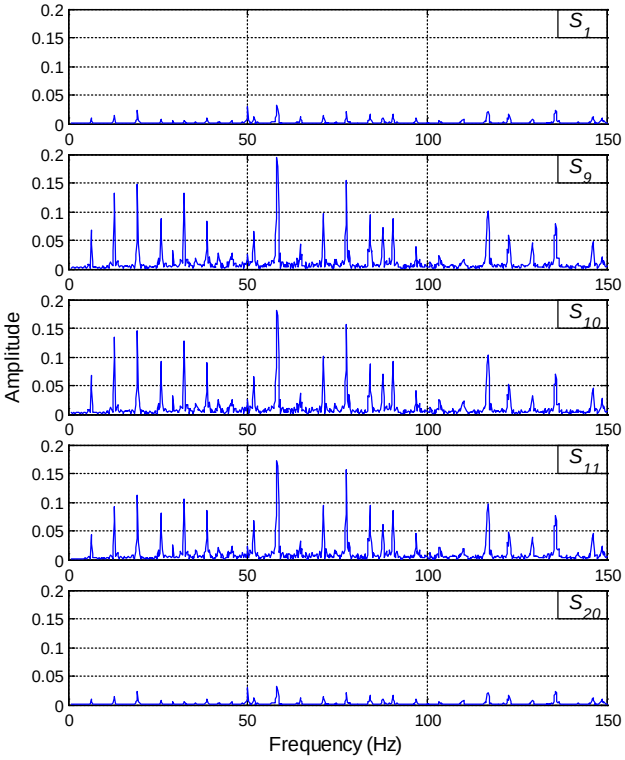

Fig. 7. Amplitude spectra of the electrostatic signals in Fig.6.

C. *ODS Measurement Results*

To calculate the ODS FRFs of the belt, sensor S_1 is selected as the reference. Fig. 8 shows the real components of the ODS FRFs at the lower frequency band (0 to 40 Hz). As illustrated in Fig.8, the peaks in the amplitude spectra appear at the same frequencies in the ODS FRFs. By connecting the peaks at the same frequency in Fig. 8, the belt ODS can be

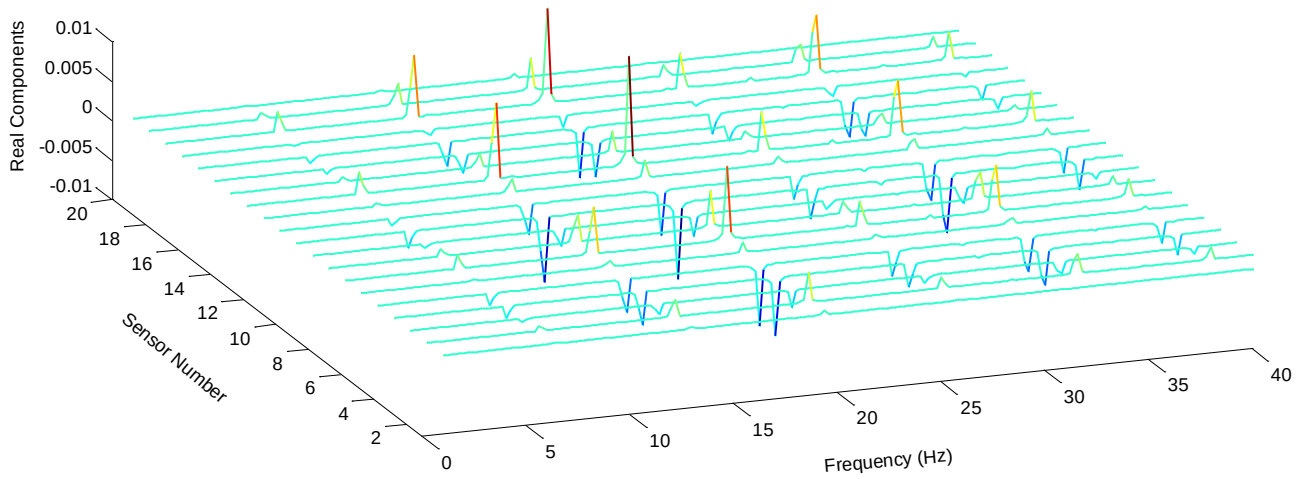

Fig. 8. The real components of the ODS FRFs.

constructed. Fig. 9 depicts the ODSs corresponding to the first four vibration modes at the resonant frequencies. Since a stretched belt is used, the fundamental vibration frequency equals the belt pass frequency [12]. The four ODSs exhibit similar deformation patterns, apart from the differences in magnitude. This result is different from the ODS measurement results for solid structures such as bridges [16], where the number of nodes (the point with minimum vibration amplitude) increases with the mode number.

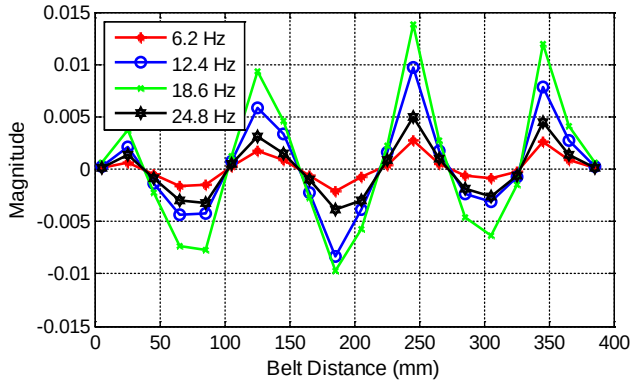

Fig. 9. The first four ODSs.

The axial motion of the belt determines that the measured ODSs translate in the belt running direction, rather than staying fixed in space. The motion of the ODS can be regarded as a travelling wave bounded by an envelope constructed with the magnitude of $H_i(\omega)$. Fig. 10 illustrates the propagating ODS of the fourth vibration mode. The other vibration modes have similar propagating ODSs bounded by envelopes with different magnitudes.

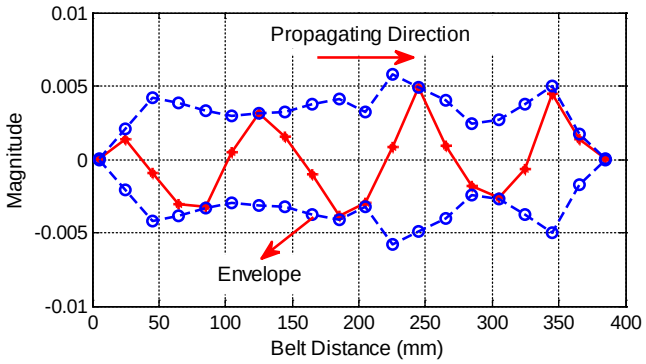

Fig. 10. Propagating ODS of the fourth vibration mode.

IV. CONCLUSIONS

This paper has presented a novel electrostatic sensing based method to measure the ODS of a power transmission belt that moves both axially and transversely. Results obtained have demonstrated that the belt vibrates at resonant frequencies, which permits the construction of the ODS using the PP method. The measured ODSs of different vibration modes exhibit similar bending shapes. Further work will be conducted to investigate the effects of belt length, type, tension and speed on the vibration and ODS characteristics. A comparison of the results with an independent reference system such as a laser vibrometer will also be carried out.

ACKNOWLEDGMENT

The authors wish to acknowledge the National Natural Science Foundation of China (No. 51375163 and No. 61573140) and the Chinese Ministry of Education (No. B13009) for providing financial support for this research. The IEEE Instrumentation and Measurement Society is also acknowledged for offering a Graduate Fellowship Award in this area of research.

REFERENCES

[1] S. Abrate, “Vibrations of belts and belt drives,” Mechanism and Machine Theory, vol. 27, no. 6, pp. 645-659, 1992.

[2] C. Xia, Y. Wu and Q. Lu, “Transversal vibration analysis of an axially moving string with unilateral constraints using the HHT method,” Mechanical Systems and Signal Processing, vol. 39, no. 1-2, pp. 471-488, 2013.

[3] B. J. Schwarz and M. H. Richardson, “Introduction to operating deflection shapes,” CSI Reliability Week, Orlando, Florida, October 1999.

[4] B. Weekes and D. Ewins, “Multi-frequency, 3D ODS measurement by continuous scan laser Doppler vibrometry,” Mechanical Systems and Signal Processing, vol. 58-59, pp. 325-339, 2015.

[5] L. Q. Chen, “Analysis and control of transverse vibrations of axially moving strings,” Applied Mechanics Reviews, vol. 58, no. 2, pp. 91-116, 2005.

[6] K. Marynowski and T. Kapitaniak, “Dynamics of axially moving continua,” International Journal of Mechanical Sciences, vol. 81, pp. 26-41, 2014.

[7] P. Catalano, F. Fucci, F. Giametta, G. L. Fianza and B. Bianchi, “Vibration analysis using a contactless acquisition system,” Proceedings of SPIE, vol. 8881, 888108, 2013.

[8] C. Xia, Y. Wu and Q. Lu, “Experimental study of the nonlinear characteristics of an axially moving string,” Journal of Vibration and Control, vol. 21, no. 16, pp. 3239-3253, 2014.

[9] A. Agnani, M. Martarelli and E. P. Tomasini, “V-belt transverse vibration measurement by means of laser Doppler vibrometry,” Proceedings of SPIE, vol.7098, 709819, 2008.

[10] R. D. Sante and G. L. Rossi, “A new approach to the measurement of transverse vibration and acoustic radiation of automotive belts using laser Doppler vibrometry and acoustic intensity techniques,” Measurement Science and Technology, vol. 12, no. 4, pp. 525–533, 2001.

[11] Y. Yan, S. J. Rodrigues and Z. Xie, “Non-contact strip speed measurement using electrostatic sensing and correlation signal-processing techniques,” Measurement Science and Technology, vol. 22, no. 7, 075103, 2011.

[12] Y. Hu, Y. Yan, L. Wang, X. Qian and X. Wang, “Simultaneous measurement of belt speed and vibration through electrostatic sensing and data fusion,” IEEE Transactions on Instrumentation and Measurement, in press.

[13] L. Wang and Y. Yan, “Mathematical modelling and experimental validation of electrostatic sensors for rotational speed measurement,” Measurement Science and Technology, vol. 25, no. 11, 115101, 2014.

[14] P. L. McHargue and M. H. Richardson, “Operating deflection shapes from time versus frequency domain measurements,” in Proceedings of the 11th International Modal Analysis Conference, Kissimmee, Florida, USA, February 1-4, 1993.

[15] W. Bae, Y. Kyong, J. Dayou, K. Park and S. Wang, “Scaling the operating deflection shapes obtained from scanning laser Doppler vibrometer,” Journal of Nondestructive Evaluation, vol. 30, no. 2, pp. 91-98, 2011.

[16] J. P. Lynch, Y. Wang, K. J. Loh, J. Yi and C. Yun, “Performance monitoring of the Geumdang Bridge using a dense network of high-resolution wireless sensors,” Smart Materials and Structures, vol. 15, no. 6, pp. 1561-1575, 2006.